Geomechanics and Engineering, *Vol. 12, No. 3 (2017) 417-439*
DOI: https://doi.org/10.12989/gae.2017.12.3.417

Bearing capacity of footing supported by geogrid encased stone columns on soft soil

Ahmet Demir [*1] and Talha Sarici [2a]

[1] *Department of Civil Engineering, Osmaniye Korkut Ata University, Karacaoğlan Campus 80000 Osmaniye Turkey*
[2] *Department of Civil Engineering, Inonu University, 44280 Malatya, Turkey*

(*Received February 25, 2016, Revised October 19, 2016, Accepted November 15, 2016*)

Abstract. The stone columns are increasingly being used as a soil improvement method for supporting a wide variety of structures (such as road embankment, buildings, storage tanks etc.) especially built on soft soil. Soil improvement by the stone column method overcomes the settlement problem and low stability. Nevertheless, stone column in very soft soils may not be functional due to insufficient lateral confinement. The required lateral confinement can be overcome by encasing the stone column with a suitable geosynthetic. Encasement of stone columns with geogrid is one of the ideal forms of improving the performance of stone columns. This paper presents the results of a series of experimental tests and numerical analysis to investigate the behavior of stone columns with and without geogrid encasement in soft clay deposits. A total of six small scale laboratory tests were carried out using circular footing with diameters of 0.05 m and 0.1 m. In addition, a well-known available software program called PLAXIS was used to numerical analysis, which was validated by the experimental tests. After good validation, detailed of parametric studies were performed. Different parameters such as bearing capacity of stone columns with and without geogrid encasement, stiffness of geogrid encasement, depth of encasement from ground level, diameter of stone columns, internal friction angle of crushed stone and lateral bulging of stone columns were analyzed. As a result of this study, stone column method can be used in the improvement of soft ground and clear development in the bearing capacity of the stone column occurs due to geogrid encasement. Moreover, the bearing capacity is effected from the diameter of the stone column, the angle of internal friction, rigidity of the encasement, and depth of encasement. Lateral bulging is minimized by geogrid encasement and effected from geogrid rigidity, depth of encasement and diameter of the stone column.

Keywords: stone column; geogrid encasement; soft clay; bearing capacity; finite element analysis; lateral bulging

1. Introduction

When existing soil may not be sufficient for supporting as a footing, properties of the existing soil or footing system must be improved. Nowadays, this problem happens often because of the increasing the urbanization dramatically. Ground improvement methods have been developed for this reason and it operates in various ways including mechanical, biological, physical, chemical

*Corresponding author, Associate Professor, Ph.D., E-mail: ahmetdemir@osmaniye.edu.tr
[a] Research Assistant, E-mail: talha.sarici@inonu.edu.tr

http://www.techno-press.org/?journal=gae&subpage=7 ISSN: 2005-307X (Print), 2092-6219 (Online)

and electrical techniques (Latifi *et al*. 2016a, b, c, Mohamad *et al*. 2013, Marto *et al*. 2012). Stone column method is one of the considerable method of soil improvement. It has been used widely over the last 30 years in many countries around the world (Black *et al*. 2007). A stone column is theoretically an upright cylinder that contains compacted granular material such as crushed stone. Soil stabilization by the stone column method overcomes the settlement problem and low stability. Another advantage of stone column method is the simplicity of its construction (Isaac and Girish 2009). There have been different studies to understand ordinary stone column behavior in the literature and it has become a popular. Studies in literature are experimental (Adalier *et al*. 2003, McKelvey *et al*. 2004, Ambily and Gandhi 2007), numerical (Mitchell and Huber 1985, Andreou and Papadopoulos 2006) and theoretical (Priebe 1995, Han and Ye 2002) studies. Adalier *et al*. (2003), conducted centrifuge tests for assessment of the stiffening effect of stone columns and its impact on the response of improved silty ground. They carried out four separate model tests with and without stone column as a free-field situation, and with a surface foundation surcharge. They proposed that stone columns could be an effective technique in the remediation of liquefaction-induced settlement of non-plastic silty deposits particularly under shallow foundations, or vertical effective stresses larger than about 45 kPa in free field conditions. McKelvey *et al*. (2004) conducted series of laboratory model tests on a group of five stone columns rested on consolidated clay bed. They used transparent material with 'clay like' properties and speswhite kaolin. Transparent material helped to visual examination of deforming granular columns during loading. They reported that bulging was significant in long columns, whereas punching was prominent in shorter columns. They also reported that the presence of the columns also greatly improved the load-carrying capacity of the soft clay bed but columns longer than about six times their diameter did not lead to further increases in the load-carrying capacity. Mitchell and Huber (1985) focused on the how well the load settlement behavior of the field load tests for stone column could be predicted and to permit estimates of the settlements of the completed structure that covered large loaded areas. They compared the field performance of stone columns by an axisymmetric finite-element model with groups of columns surrounding the central column replaced by a ring of stone material having equivalent thickness. Andreou and Papadopoulos (2006) carried out to finite element analysis based on unit cell concept. They investigated to influence of different factors and concluded some practical results on the design of stone columns. Applied load in the ground, area replacement factor, friction angle of the gravel and undrained shear strength of the soil, on the horizontal displacements were analyzed by authors.

Priebe (1995) suggested a method to estimate the settlement of foundation resting on the infinite grid of stone columns based on unit cell concept. Some researchers also have been used unit cell concept (Barksdale and Bachus 1983, Goughnour 1983, Sathish *et al*. 1997). In this concept, the area of the stone column pattern represented by a single column, depending on column spacing and this area is considered for the analysis. In addition, it is supposed that lateral deformation in soil at the boundary of unit cell is zero. This concept has been useful to researchers because experimental studies, especially small-scale, have been quicker and becomes meaningful. The undrained shear strength of the surrounding soil of stone column is generally important factor for the durability of stone columns and disintegration of the granular material used for making stone column. The range of 5-15 kPa shear strength for the surrounding soil of stone column is suggested as a minimum value (Wehr 2006, Madhav and Miura 1994, Priebe 1995, Wood *et al*. 2000).

Below this range of shear strength, the lateral confinement provided by surrounding natural soil may not be sufficient to prevent column failure and excessive radial expansion may occur. In the last years, it has been trying to resolve this restriction by geosynthetic encasement to provide the required lateral support to columns installed in extremely soft soils (Gniel and Bouazza 2009). Geosynthetic encased stone columns is stiffer, stronger and more resistant to disintegration than ordinary stone column. However, a limited number of studies are available at the present time relating to the bearing capacity of circular footing supported by a geogrid encased stone columns on soft soil (Gniel and Bouazza 2009, 2010). Gniel and Bouazza (2009) carried out series of small-scale laboratory test. They focused on the behavior of geogrid-encased columns. They investigated the effect of varying the length of encasement and compared the different encasement length with fully encased column. Additionally, single column was compared to group column. They presented that partially geogrid encased stone column's vertical strain decreases with increasing encased length for both single and group stone columns. Lateral bulging of the stone column was observed to occur directly beneath the base of the encasement. They have achieved a result in this article that, fully encased stone columns are stiffer than all other conditions of the stone column test. Marto *et al*. (2013) conducted numerical analysis by using finite element software PLAXIS for simulating the behavior of ordinary and geogrid encased stone columns in soft clay soil. They presented settlement and bearing capacity of ordinary and geogrid encased stone columns. They reported that load-carrying capacity of the stone column could be increased by the increase of the diameter of the column. They also found that load-carrying capacity and stiffness of the stone column can be increased by all-round encasement by geogrid, geogrid encasement minimized the lateral bulging of stone column and load-carrying capacity of stone columns can be increased by using stiffer geogrid encasement.

According to the author's knowledge, when used the geogrid encasement on stone columns, the effect of the geogrid encasement on the bearing capacity behavior of footings on soft clay deposits has not yet been investigated extensively in the geotechnical engineering. This study attempts to provide a better understanding of the behavior circular footing resting on geogrid encased stone columns on soft clay under vertical loadings. For this purpose, firstly, experimental studies have been carried out to define the ultimate load, and then, the load-settlement curves have been plotted. Secondly, the effectiveness of geogrid encasement on the stone columns is investigated through parametric study carried out by finite element analysis. Before conducting the finite element analysis, the validity of the numerical model was checked using laboratory model tests. The influence of the parameters such as diameter of stone column, crushed stone friction angle, the rigidity of geogrid, length of geogrid reinforcement, lateral bulging of stone column, percentage reduction in settlement, percentage reduction in lateral bulging and comparison with existing studies were explored.

2. Test equipment and materials

2.1 General

The experimental program was carried out using the facility in the Geotechnical Laboratory of the Civil Engineering Department at the University of Osmaniye Korkut Ata. The facility and a typical model are given in Fig. 1.

2.2 Test setup and loading arrangements

Loading tests were performed using two different model rigid circular footings (diameter of footings are 5 cm and 10 cm) fabricated from mild steel with a thickness of 15 mm. For all tests,

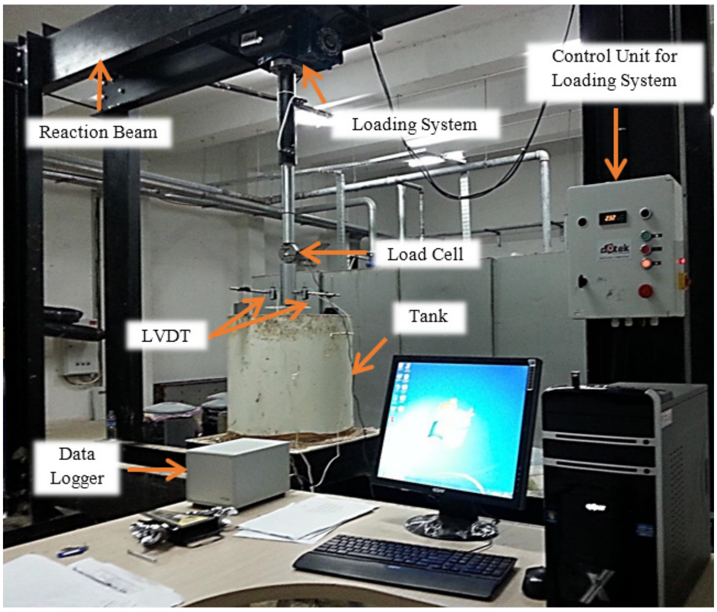

(a)

(b)

Fig. 1 Test set-up: (a) overview; (b) circular footing

loading was done only for stone column area. Tests were conducted in a circular steel tank with dimensions of 60 cm (diameter) and 60 cm (depth). The bottom and vertical edges of the tank were made up using steel plates with a thickness of 12 mm to avoid lateral yielding during the soil placement and loading of the model footing. The boundary distances were greater than the footing diameter. It was observed that the extent of failure zones was not more than the footing geometry during the tests, and the frictional effect was insignificant to affect the results of model tests.

The model footings were loaded vertically by a motorized gearbox arrangement attached to loading frame located above the tank. The loading system is based on displacement control and speed of displacement of setup is controlled by DC motor. The speed of the motor was adjusted by the speed control unit to give a vertical displacement rate of 2.33 mm/min. Load and displacement measurements were taken using a load cell and two LVTD's of 0.01 mm sensitivity suitably installed between the jack and the model footing. A schematic diagram of the test setup is given in Fig. 2.

2.3 The soil properties

2.3.1 Clay and stone column material

The clay soil used was obtained from locally available soil, which two test pit excavations were performed, in the Adana Metropolitan Municipality's (AMM) Water Treatment Facility Center (WTFC) located in west part of Adana, Turkey. Surface clay was excavated after removal of vegetation, air-dried, and pulverized. The clay was sieved through 2.00 mm sieve to remove the coarser fraction and for easy processing and uniform water content.

After conducting required conventional laboratory tests (sieve and hydrometer analysis, moisture content analysis, unit weight analysis, liquid and plastic limit analyses, unconfined

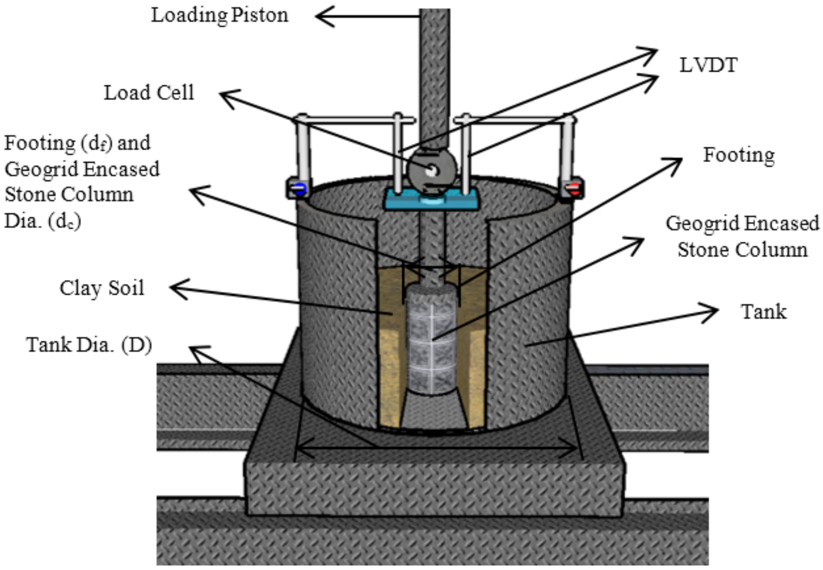

Fig. 2 General layout of apparatus for the model test

compression test) the soil was prepared for model tests. The clay soil was identified as high plasticity inorganic clay, CH according to the unified soil classification system. The values of liquid limit, plastic limit and plasticity index of soft soil were obtained as 55%, 22% and 33%, respectively. The values of specific gravity of clay soil were obtained as 26.0 kN/m^3. The characteristics of the soft soil determined through an extensive testing program that consisted of a combination of laboratory and in situ tests were given in detail by Demir (2011). The properties of clay use in experimental work are shown in the Table 1.

A series of unconfined compressive strength (UCS) tests were carried out on cylindrical specimen with 38 mm diameter and 76 mm height to determine the moisture content corresponding to 15 kPa undrained shear strength of the clay. The results of variation of undrained shear strength with water content are given in Fig. 3. Water content of the clay was selected as a 35% and this amount was kept the same in all tests.

The stone columns were formed from crushed stones, which was classified GP and crushed stones (aggregates) of sizes between 10 and 2 mm. The gradation curve was selected based on

Table 1 Properties of clay

Parameters	Values
Specific gravity (G_s)	2.6
Liquid limit (%) (LL)	55
Plastic limit (%) (PL)	22
Classification	CH
Water content (%) (ω)	35
Natural density (kN/m^3) (γ_n)	18.2
Undrained shear strength of clay (kPa) (c_u)	12

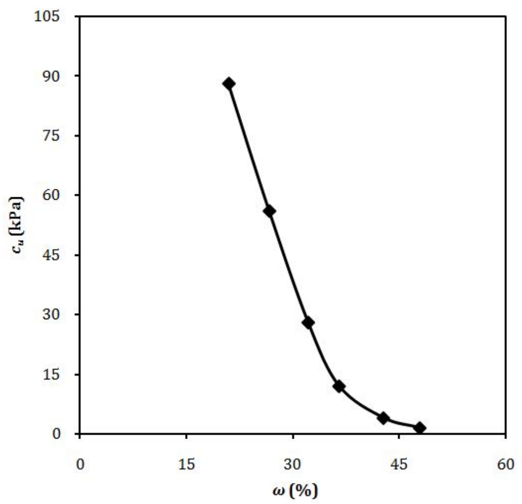

Fig. 3 Variation of undrained shear strength with water content

previous studies such as Murugesan and Rajagopal (2009). The particle size distribution for stone column and clay materials are indicated in Fig. 4, respectively. The maximum dry unit weight ($\gamma_{k\max}$) and minimum dry unit weight ($\gamma_{k\min}$) of the aggregate are 16.9 and 15.2 kN/m^3, respectively. Other properties of the aggregate for the stone column are given in Table 2. The angle of internal friction was determined using a large scale direct shear box (45 × 45 × 20 cm). The crushed stones were compacted to a density of 16.30 kN/m^3, which could be achieved while constructing the stone columns for the experiments and sheared at a constant rate of 1.25 mm/min under normal pressures of 50, 100, and 150 kPa.

2.3.2 Reinforcement material

Bulging is one of the most common failure mechanisms for granular piles (Madhav and Miura 1994). In this failure, the granular material in the top portion of the pile is displaced laterally into the soil while the composite ground settles under compressive load. The load transfer to the surrounding clay depends on the deformed shape of the pile. The varying diameter of the pile over a certain length plays a vital role in load transfer (Wood *et al*. 2000). Bulging can be avoided by

Table 2 Properties of crushed stones used as stone column

Parameters	Values
Specific gravity (G_s)	2.85
Density (kN/m^3) (γ_n)	16.3
Maximum dry unit weight (kN/m^3) ($\gamma_{\max}$)	16.9
Minimum dry unit weight (kN/m^3) ($\gamma_{\min}$)	15.2
Internal friction angle (Degree) (ϕ)	44^0
Uniformity coefficient (C_u)	1.67
Coefficient of curvature (C_c)	1.10
Classification	GP

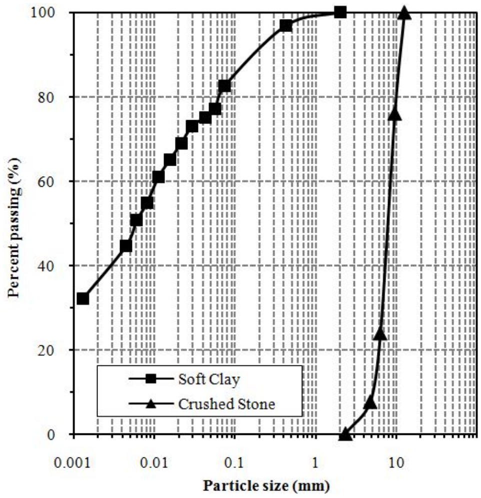

Fig. 4 Particle size distribution for soft clay and stone column materials

Table 3 Properties of geogrid encasement

Parameters	Values
Type of material	Polypropylene
Weight per unit area (g/m^2)	200
Max. tensile strength, md/cmd* (kN/m)	≥30 / ≥30
Tensile strength of 2% elongation, md/cmd* (kN/m)	12 / 12
Tensile strength of 5% elongation, md/cmd* (kN/m)	24 / 24
Aperture (mm x mm)	40 × 40

using concrete plugs or cement grout (Rao and Bhandari 1980). Reinforcing granular piles with geogrids also prevents bulging (Kabir and Alamgir 1989). In a granular pile enveloped by a geosynthetic, bulging is reduced and load-carrying capacity increased (Adayat and Hanna 1991). In this study, geogrid was used for encasement of the stone column. Stone column was restrained by the geogrid encasement to provide additional confinement for improved stone column performance. Geogrid used in the experimental study, is commercially available from GEOPLAS Company. The properties of geogrid taken from GEOPLAS Company are shown in the Table 3.

2.4 Experimental procedure

Three pilot tests (unreinforced clay bed, stone column reinforced clay bed and geogrid encased stone column reinforced clay bed) were conducted to learn how experiments done in the best conditions. For preparing the soft clay soil bed, a circular tank of 60 cm diameter and 60 cm height was used in all the tests. Tests have been conducted in a clay bed prepared at about moisture content of 35% to obtain required shear strength value, which is suggested as a minimum value of 5-15 kPa for the surrounding soil of stone column (Wehr 2006, Madhav and Miura 1994, Priebe 1995, Wood *et al*. 2000). For preparation of each test bed, the soft clay soil pulverized was thoroughly mixed with required amount of water (ω_n = 35%). To achieve uniform moisture distribution, the wet soil was placed in airtight plastic containers and stored for 2 to 3 days before being used in experimental study. Before filling the test tank, lubricating oil was smeared along the inner surface of test tank wall to reduce friction between clay and test tank wall. The soft clay soil was placed in the test tank in layers with small quantities, which were tapped gently with a special hammer and spread uniformly. Soft soil was filled in the test tank in layers with measured quantity by weight. The surface of each layer was provided with uniform compaction with a special hammer to achieve a 5 cm height, uniform density and required shear strength as per requirement. After the test tank was filled to layer of 5 cm height, pocket penetrometer test was carried out. Unconfined compressive strength also conducted in pilot test to verify the subsequent pocket penetrometer tests. Water content of soft clay soil was also determined at different locations and found to be almost uniform with 1% variation. The procedure was repeated until the soft clay soil bed is completed to the full height. In all test full height of the soft clay soil is 25 cm. The degree of saturation was also calculated by taking undisturbed samples from the tank in tests. The average degree of saturation by this placement method was achieved as about 93.0%.

Based on the pilot tests, it was decided to use the replacement method (Gniel and Bouazza 2010) to construct the columns in all tests. The drill rig and a thin wall tube supported and located in the two way (horizontally) controlled steel frame were used to construct the model columns. In order to minimize disturbance to the surrounding clay during the penetration of the tube, lubricating oil was smeared on the outside of the tube before the formation of every other column. A seamless tube of 5 and 10 cm outer diameter and wall thickness 2 mm was pushed into the soft clay soil at the center of the tank up to the bottom. Outer diameter of the tube equal to the diameter of the stone columns. The soft clay soil within the tube was removed using a drill rig. During this process, small quantities of soft clay soil were removed to avoid suction effect. Crushed stones were charged into the tube and compacted with special hammer, which is suitable for tube. This process was done in layers of 5 cm height. Based on the pilot tests, this compaction effort was selected to eliminate significant disturbance of the surrounding soft clay soil. Density of the stone column built with crushed stone was found to be 16.30 kN/m^3. Upon reaching the layer of 5 cm height, the tube is slowly withdrawn. This construction stages was repeated until the column is completed to the full height. In all test full height of the stone column is 25 cm. To construct single stone columns, H/d_c ratio (height of stone column/diameter of stone column) of 2.5 and 5 has been used which is required to develop the full maximum axial stress on the column (Mitra and Chattopadhyay 1999). The case of geogrid reinforced stone column tests, encasement was provided around the tube that was not smeared the lubricating oil. As in the unreinforced stone column construction, tube that was smeared the lubricating oil was pushed into the soft clay soil until the bottom of the tank. Afterward, this tube is slowly withdrawn and the tube along with the geosynthetic encasement was slowly pushed into the soft clay soil at the center of the tank up to the bottom. Other construction stages were done as in the unreinforced stone column construction. For each test, the load-displacement readings were recorded with a twenty-nine-channel data-logger unit (ALMEMO 5690 series Autonomous Data Acquisition System) and converted to produce values of the displacement at ground level and load using The AMR WinControl software package that has been specially developed for data acquisition and measured data processing with ALMEMO equipment, on a PC.

In experimental study, the behavior of circular footing rested on unreinforced clay deposits, clay deposits stabilized with stone columns and clay deposits stabilized with geogrid encasement stone columns was investigated using small scale laboratory tests. Summary of experimental study is shown in the Table 4.

Table 4 Summary of experimental study

Test series	Test number	Test description	Diameter of the footing, d_f (cm)	Diameter of the stone column, d_c (cm)
I	1	Unimprovement case	5	-
	2		10	-
II	3	Stone column without geogrid reinforcement case	5	5
	4		10	10
III	5	Geogrid encased stone column case	5	5
	6		10	10

3. Finite element modeling

The FE analyses have been performed to obtain the load–displacement curves for rigid circular footings resting on soft clay soil with and without improved as the same model geometries as in the tests. FE analysis is a powerful mathematical tool that makes it possible to solve complex engineering problems. The finite-element method is a well-established numerical analysis technique used widely in many civil-engineering applications for research and the solution of real engineering problems. The constitutive behavior of the soils can be successfully modelled with numerical analyses. The finite-element method is one of the mathematical methods in which continuous media is divided into finite elements with different geometries. It provides the advantage of idealizing the material behavior of the soil, which is non-linear with plastic deformations and is stress-path dependent, in a more rational manner. The finite-element method can also be particularly useful for identifying the patterns of deformations and stress distribution during deformation and at the ultimate state (Demir and Ok 2015). Numerical analyses were carried out by using the Plaxis 2D-V2011 software. It is based on a finite element method and specially developed for the analysis of geotechnical engineering problems (Brinkgreve *et al*. 2004). Finite element model was simulated using 15-node triangular elements. Because of the symmetry of the test tank used in experimental study, axisymmetric modelling is considered in the numerical analyses (Murugesan and Rajagopal 2006, Yoo and Kim 2009).

The Plaxis software incorporates a fully automatic mesh-generation procedure, in which the geometry is divided into elements of the basic element type, and compatible structural elements. In order to obtain the most suitable mesh for the present study, preliminary analysis using the five available levels of global mesh coarseness (ranging from very coarse to very fine) were performed. It was decided to use the medium mesh in all the analyses, since there is not too much difference in the results for different mesh configurations.

Finite element model used in analysis is shown in Fig. 5 and typical mesh configurations in the finite element analyses are shown in Fig. 6. For all analysis, loading was done only for stone column area. An elastic-plastic Mohr Coulomb (MC) model was chosen to simulate clay soil and stone column behavior. The soil parameters used in the main investigation, which were obtained from conventional laboratory tests, are shown in Table 5 (ASTM D 2435-96 1998, ASTM D 3080-98 2003, ASTM D2166 2003).

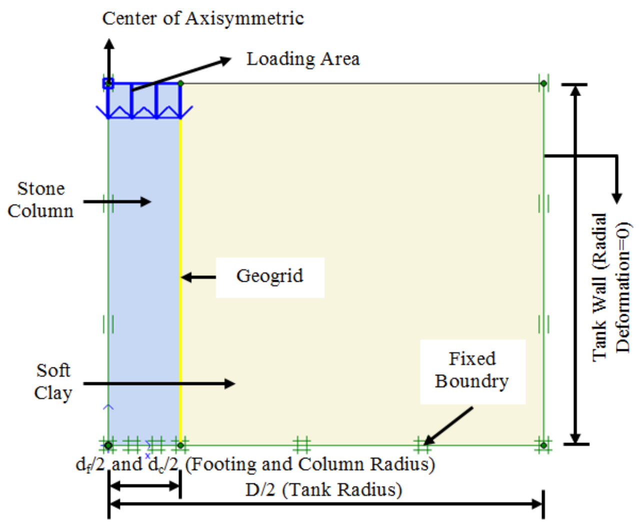

Fig. 5 Finite element model

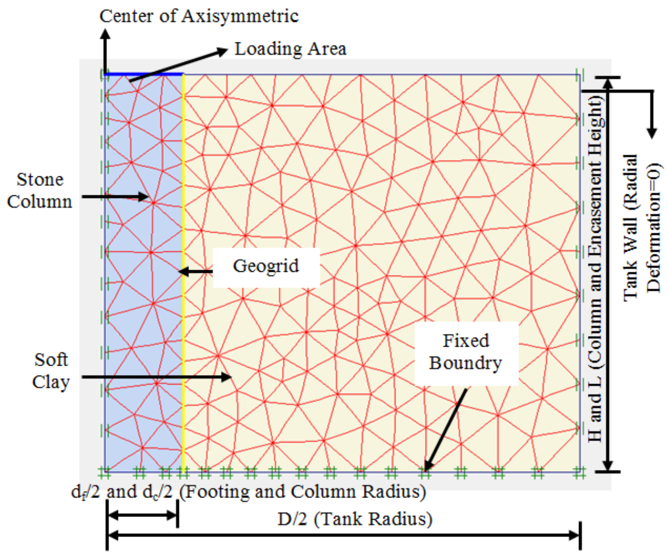

Fig. 6 Typical mesh configurations used in the FE analyses

Table 5 Soil properties used in FE analyses

Parameters	Clay value	Stone column value
Unit weight, γ (kN/m^3)	18	21
Loading stiffness, E_u (kN/m^2)	290	65000
Cohesion, c (kN/m^2)	15	1
Poisson's ratio, v	0.35	0.3
Friction angle, ϕ (degrees)	1°	45°
Dilatancy angle, ψ (degrees) (ϕ - 30°)	0	15°

4. Validation of finite element approach with experimental results

Experimental and numerical studies were performed to obtain bearing capacity-settlement ratio curves for rigid circular footings resting on soft clay soil with and without improved. Results of the experimental and numerical studies for the same condition were compared with each other. Thus, the accuracy of the finite element model has been approved. The bearing capacities (q)-settlement ratio curves, both of numerical and experimental analysis, are presented in Fig. 7. The horizontal and vertical axes show the bearing capacities and the settlement ratios, respectively. The settlement ratio (s/d_f) is defined as the ratio of the footing settlement (s) to the footing diameter (d_f), expressed as a percentage. It is clear from the figures that the vertical displacements predicted by the numerical analysis are in very good agreement with the experimental results. The settlement pattern generally resembles a typical local shear failure and the maximum bearing capacity was not clearly well defined.

Fig. 7(a) shows results of experimental study conducted using diameter of 5 cm circular footing (so stone column has a 5 cm diameter) and its numerical analysis while Fig. 7(b) shows results of experimental study conducted using diameters of 10 cm circular footing (so stone column has a 10 cm diameter) and its numerical analysis. As seen from the Figs. 7(a) and (b), result of experimental study and numerical analysis for different conditions such as unimprovement case (C), stone column without geogrid reinforcement case (SC) and geogrid encased case (GESC) are presented.

It is shown from the Fig. 7 that stone column layer helps to increase the bearing capacity of the footing and decreases the settlement allowable load since the stone column layer is stiffer and stronger than the natural clay. The partial replacement of the soil with the granular-fill layer (stone column) results in a redistribution of the applied load to a wider area and so minimizing the stress concentration and achieving an improved distribution of induced stress. For this reason, the bearing capacity can be improved while the footing settlement is reduced. It is observed that the load-settlement curve is rounded and becomes steeper and takes on an almost a linear shape. A peak load is never observed and no definite failure point can be established. The mode of failure

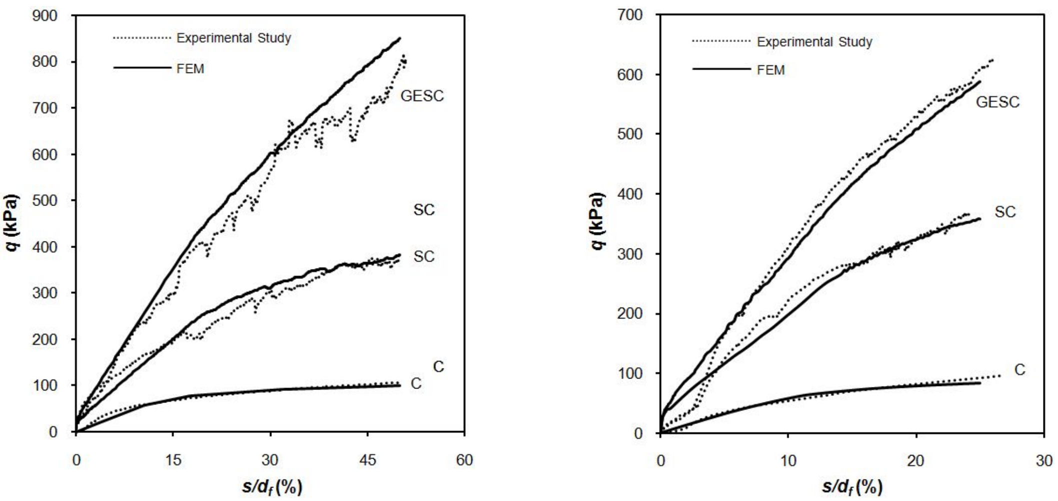

(a) d_c = 5 cm (b) d_c = 10 cm

Fig. 7 Comparison between numerical analysis and experimental study for different conditions

Table 6 Limiting axial stress values obtained from experimental and numerical studies

Test series	Test number	Test description	d_f (cm)	d_c (cm)	Numerical analysis (kPa)	Experimental study (kPa)
I	1	Unimprovement case	5	-	54.3	58.5
	2		10	-	57.9	54.1
II	3	Stone column without geogrid reinforcement case	5	5	142.3	161.9
	4		10	10	198.9	222.5
III	5	Geogrid encased stone column case	5	5	244.5	233.6
	6		10	10	291.7	310.9

can be described as a local shear failure. As seen from the figures that geogrid encasement improves the performance of stone column.

The limiting axial stress value may be defined based on the settlement such as that which causes a settlement equal to 10% of the column diameter (Malarvizhi and Ilamparuthi 2004). Limiting axial stress values obtained from experimental and numerical studies are summarized in Table 6.

As seen from the Table 6, limiting axial stress values predicted by the numerical analysis are in very good agreement with the experimental results. In addition, it is clear from the results that stone column increase the limiting axial stress and geogrid encasement increase the limiting axial stress performance of the stone column. In addition, as seen from the Table 6 and Fig. 7, limiting axial stress of all test series using the diameters of 10 cm circular footing are higher than diameters of 5 cm circular footing.

5. Details of the parametric studies

After achieving a good consistency between numerical and experimental studies, the numerical analyses were continued to investigate different parameters such as effect of diameter of stone column, crushed stone friction angle, the rigidity of geogrid and length of geogrid reinforcement. In addition, lateral bulging of stone column, percentage reduction in settlement, percentage reduction in lateral bulging and comparison with existing studies were explored.

5.1 Effect of stone column diameter

When examining effect of the column diameter, undrained shear strength of clay and tank diameter were kept constant. For all analysis, loading was done only for stone column area. Fig. 8 shows a relation between diameter ratio (column diameter/tank diameter = d_c/D) and limiting axial stress (q_u). Lower limit is the bearing capacity of unreinforced clay deposit. It is clear from the figure that limiting axial stress of stone column (SC) and geogrid encased stone column (GESC) increases by the increases of the column diameter.

5.2 Effect of crushed stone friction angle

Stone column was built using crushed stone and crushed stones properties directly affect the behavior of the stone columns. Therefore, effect of crushed stone friction angle was studied. For

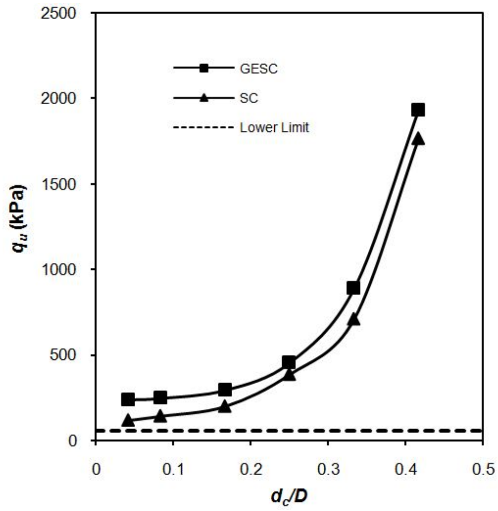

Fig. 8 Effect of diameter of stone column

this investigation, column diameter, undrained shear strength of clay and tank diameter were kept constant. Based on the results, limiting axial stress versus for different angles of internal friction of crushed stones is presented in Fig. 9. Fig. 9(a) shows results of numerical analysis conducted using diameters of 5 cm circular footing (so stone column has a 5 cm diameter) while Fig. 9(b) shows results of numerical analysis conducted using diameters of 10 cm circular footing (so stone column has a 10 cm diameter). As can be seen from the Fig. 9 that limiting axial stress increases with increases in crushed stone friction angle.

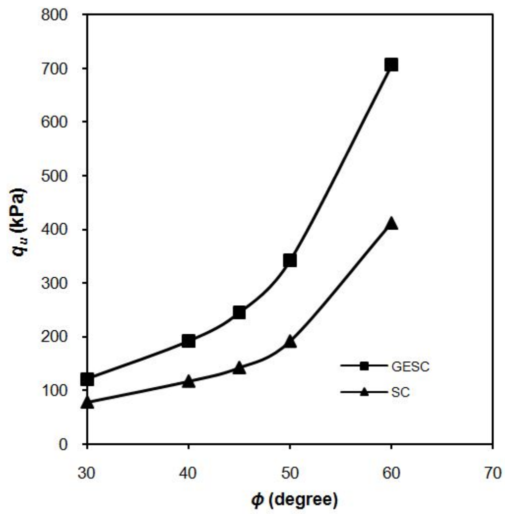

(a) d_c = 5 cm

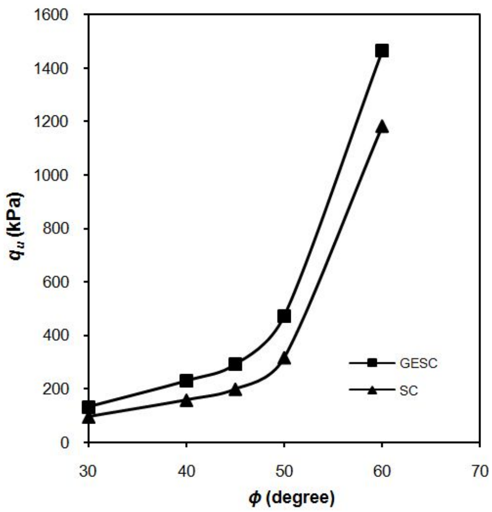

(b) d_c = 10 cm

Fig. 9 Effect of crushed stone friction angle

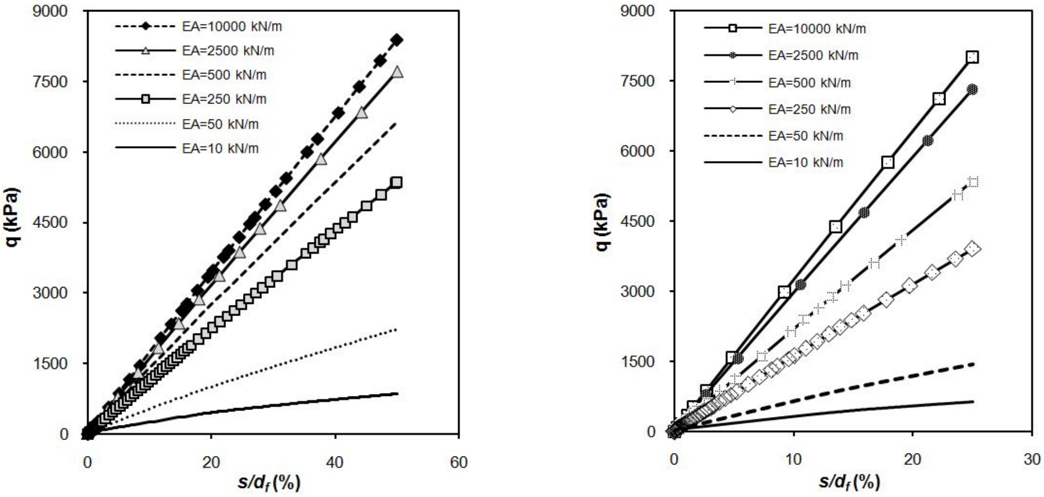

(a) d_c = 5 cm (b) d_c = 10 cm

Fig. 10 Effect of geogrid rigidity

5.3 Effect of the geogrid rigidity

As seen from the experimental and numerical studies, geogrid encasement improves the performance of stone column. In this part, effect of the geogrid rigidity on the behavior of stone columns was investigated and it is presented in Fig. 10. For this investigation, column diameter, undrained shear strength of clay and tank diameter were kept constant. The rigidities of geogrid reinforcement were taken as EA = 10, 50, 250, 500, 2500, 10000 kN/m. It is observed from these parametric studies that the stiffness of the geosynthetic reinforcement significantly affects the behavior of geogrid-reinforced stone column resting on soft soil. It is clear from the Fig. 10 that bearing capacity increases by the increase of the geogrid rigidity.

5.4 Effect of geogrid reinforcement length

Geogrid encasement length was evaluated for different L/H ratio. L is the geogrid encasement length from the top portion of stone column. H is the stone column length, which is 25 cm in all numerical analysis. Geogrid stiffness kept constant which is the 10 kN/m while L/H ratio is variable. It is clear from the Fig. 11 that bearing capacity decreases by the decrease of the geogrid encasement length.

5.5 Lateral bulging of stone columns

Bulging is one of the failure modes of the stone columns. As previously mentioned, to resolve this problem, stone column is wrapped using geogrid. To attract attention to this situation, in numerical analysis, lateral bulging of the stone column with and without geogrid encasement were investigated. Lateral bulging was measured when 25 mm axial displacement occurs. Lateral bulging at various depths is presented in terms of the increase in radius 'Δ_z' at different depths normalized with original radius of the stone column (d_c). This value is also equal to the hoop strain (ε_θ) in percent (because $\varepsilon_\theta = u/d_c$ in which 'u' is the radial displacement). Fig. 12 shows a relation

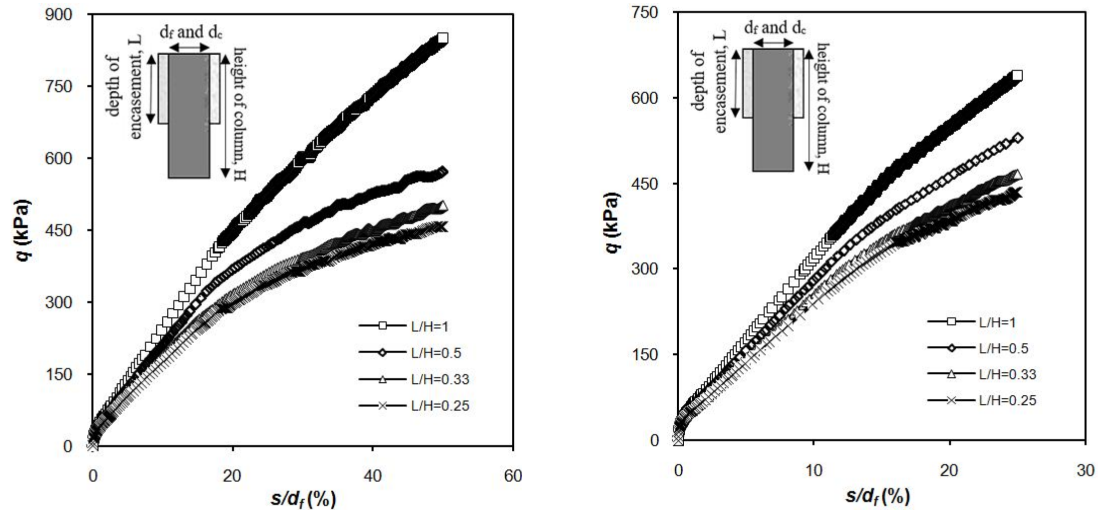

(a) d_c = 5 cm (b) d_c = 10 cm

Fig. 11 Effect of geogrid reinforcement length

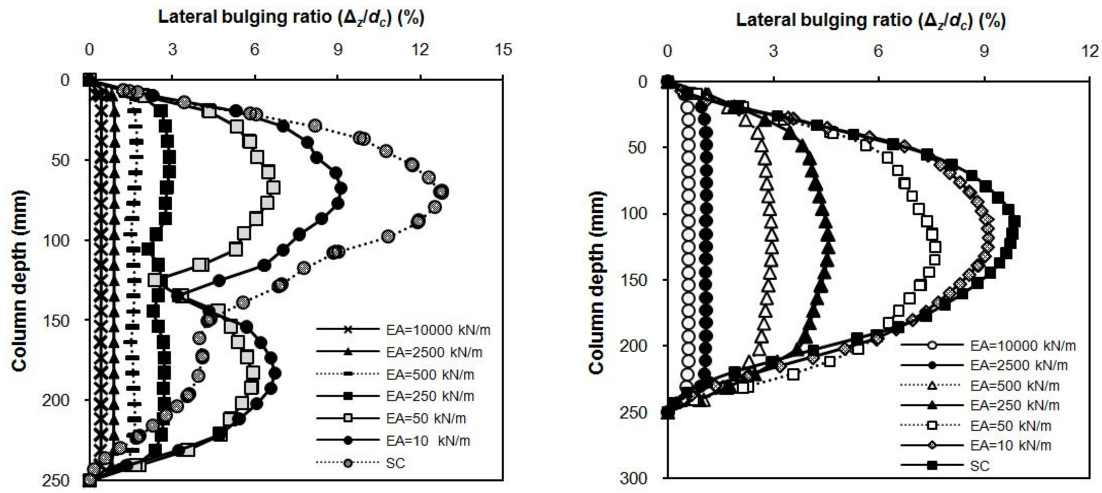

(a) d_c = 5 cm (b) d_c = 10 cm

Fig. 12 Lateral bulging of stone columns for different rigidity of geogrid

between lateral bulging ratio (ratio between the amount of lateral bulging and diameter of stone column) and column depth for different geogrid rigidity and diameter of column. As understood from the Fig. 12 that geogrid encasement reduces lateral bulging and lateral bulging of stone column decreases with increase in rigidity of geogrid.

It was observed that, maximum value of bulging of stone column occurs at depth of almost 1-2 times the diameter of stone column from the ground surface. Therefore, only the top portion of the stone column may be improving the bulging performance. Therefore, influence of the encasement depth on the bulging behavior of the stone columns was investigated. Analyses were performed

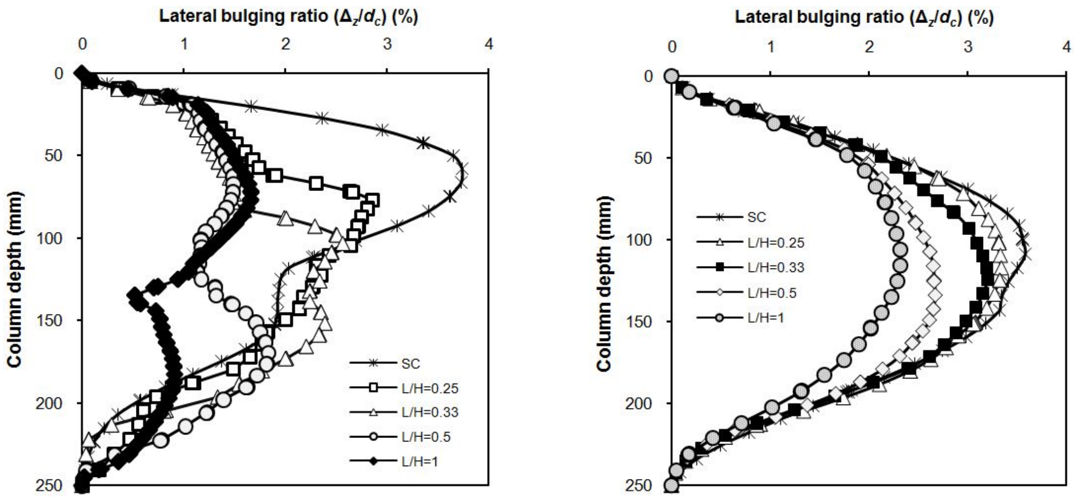

(a) d_c = 5 cm (b) d_c = 10 cm

Fig. 13 Lateral bulging of stone columns for different *L*/*H* ratio

under a particular vertical pressure of 200 kPa using encasement rigidity of 10 kN/m and by varying the depth of encasement from the ground level. As can be seen from the Fig. 13, relation between lateral bulging ratio and column depth for different *L*/*H* ratio are presented. For both diameter of stone column, it is clear from the Fig. 13 that the lateral bulging of stone column decreases as the encasement depth increases.

5.6 Percentage reduction in settlement (*PRS*)

The improved performance in settlement was quantified based on the percentage reduction in settlement of the stone column. The improvement due to the provision of an encased stone column for different rigidity, in terms of reduction in footing settlement, can be quantified through the parameter settlement reduction factor, which is defined as

$$PRS = \frac{S_u - S_r}{S_u} \times 100 \tag{1}$$

wherein, S_u is the settlement of the unreinforced stone column at a limiting axial stress and S_r is the settlement of the encased stone column with different rigidity at the same pressure. This settlement reduction factor is same as the parameter used by Murugesan and Rajagopal (2006).

PRS of reinforced stone columns over that of the unreinforced stone column for different rigidity values of geogrid under a limiting axial stress is shown in Fig. 14 for two diameters of stone column. The rigidities of geogrid reinforcement were taken as EA = 0 (uncased stone column), 10, 20, 40, 50, 80, 160, 250, 500, 2500 kN/m. It is observed that percentage reduction in settlement is heavily dependent on geogrid rigidity and depth of encasement from the ground level. Performance improvement of stone column increases almost linearly EA = 0 kN/m to EA = 160-250 kN/m. After rigidity of EA = 160-250 kN/m performance improvement of stone column remains constant.

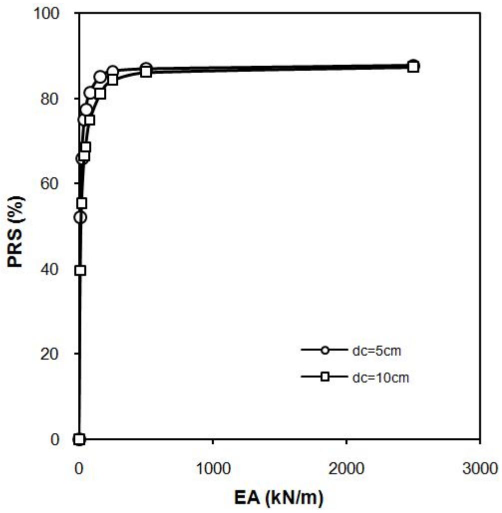

Fig. 14 Percentage reduction in settlement with increasing geogrid rigidity

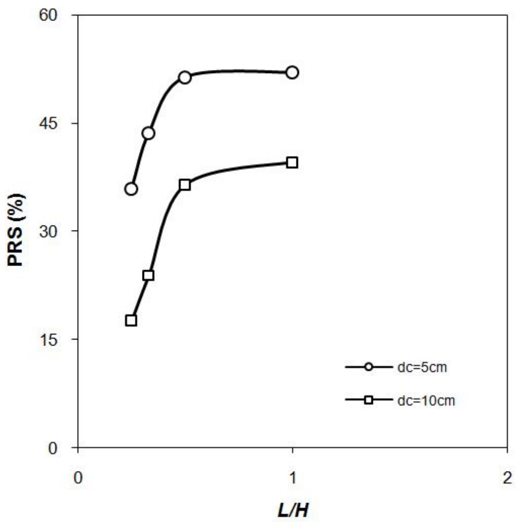

Fig. 15 Percentage reduction in settlement with increasing *L*/*H*

PRS of reinforced stone columns over that of the unreinforced stone column for different *L*/*H* ratio of geogrid encasement under a limiting axial stress is shown in Fig. 15 for two diameters of stone column. Geogrid stiffness kept constant which is the 10 kN/m while *L*/*H* ratio is variable (0.25, 0.33, 0.5, 1). In addition, performance improvement of stone column increases with increases in *L*/*H*. It is clear that the confinement at the top portion (where predominant lateral bulging occurs) of the stone column is adequate for improved performance. As can be seen from the Figs. 14 and 15, percentage reduction in settlement for 5 cm diameter of stone column is higher than 10 cm diameter of stone column.

5.7 Percentage reduction in lateral bulging (PRB)

The improved performance in lateral bulging was quantified based on the percentage reduction in maximum lateral bulging of the stone column. The improvement due to the provision of a encased stone column for different rigidity, in terms of reduction in maximum lateral bulging, can be quantified through the parameter lateral bulging reduction factor which is defined as

$$PRB = \left\{ \left[\left(\frac{\Delta_z}{d_c} \right)_u - \left(\frac{\Delta_z}{d_c} \right)_r \right] \div \left(\frac{\Delta_z}{d_c} \right)_u \right\} \times 100 \quad (2)$$

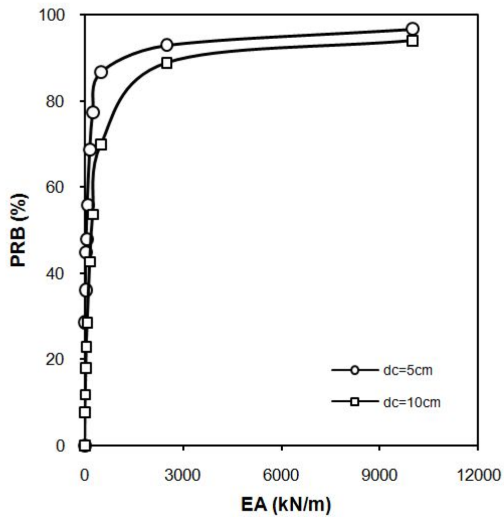

Fig. 16 Percentage reduction in lateral bulging with increasing geogrid rigidity

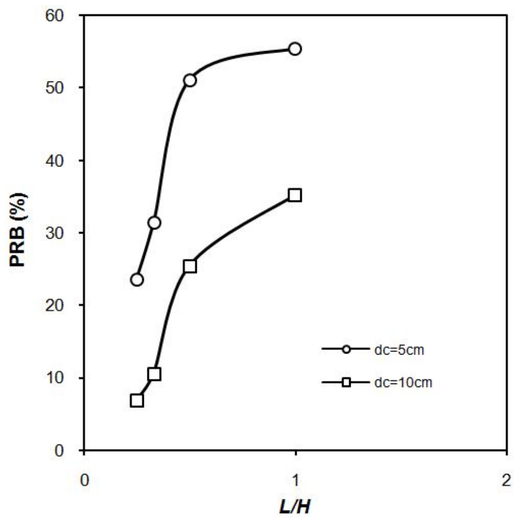

Fig. 17 Percentage reduction in lateral bulging with increasing *L*/*H* ratio

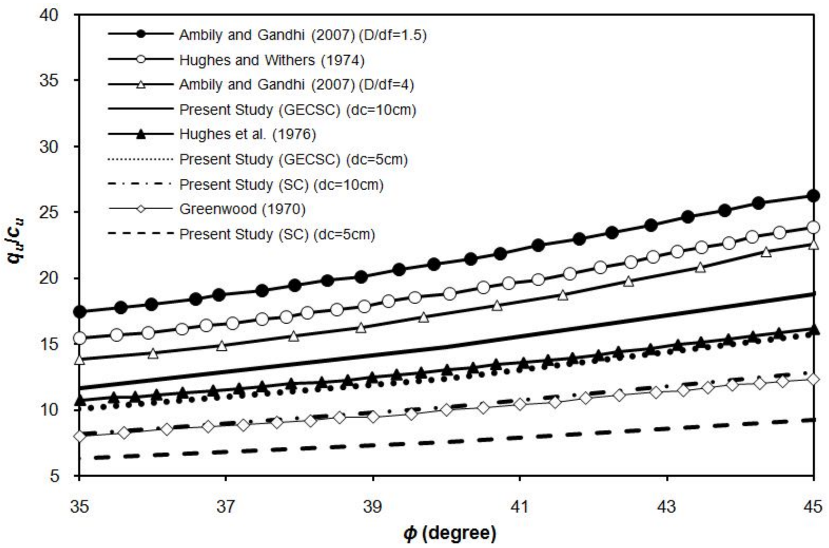

Fig. 18 Comparison between present and existing studies

wherein, $(\Delta_z/d_c)_u$ is the maximum lateral bulging ratio of the unreinforced stone column at a limiting axial stress and $(\Delta_z/d_c)_r$ is the maximum lateral bulging ratio of the encased stone column with different rigidity at the same pressure. This settlement reduction factor is same as the parameter used by Murugesan and Rajagopal (2006). The rigidities of geogrid reinforcement were taken as EA = 0 (uncased stone column), 10, 20, 40, 50, 80, 160, 250, 500, 2500, 10000 kN/m. The reduction in maximum lateral bulging (occurring near the top portion) due to the encasement of various geogrid rigidity values is shown in Fig. 16 for different stone columns diameters. It is clear that, as the stiffness of the encasement increases, the maximum bulging is observed decreases due to the effects of lateral confinement. As can be seen from the Fig. 16 percentage reduction in lateral bulging for 5 cm diameter of stone column is higher than 10 cm diameter of stone column.

PRB of reinforced stone columns over that of the unreinforced stone column for different *L*/*H* ratio of geogrid encasement is shown in Fig. 17 at an applied pressure of 200 kPa. Geogrid stiffness kept constant which is the 10 kN/m while *L*/*H* ratio is variable (0.25, 0.33, 0.5, 1). For both diameter of stone column, it is clear from the Fig. 17 that PRB increases as the *L*/*H* ratio increases.

5.8 Comparison with existing studies

The relationship between present and existing studies was investigated. To specify this relationship, the friction angle for the granular material (ϕ) with the ratio of the limiting axial stress stone column (q_u) to the shear strength of surrounding clay (c_u) are presented in Fig. 18. Existing studies were prepared by Ambily and Gandhi (2007) (spacing between columns/diameter of column = 1.5), Hughes and Withers (1974), Ambily and Gandhi (2007) (spacing between columns/diameter of column = 4), Hughes *et al*. (1976), Greenwood (1970).

The existing studies (except Ambily and Gandhi 2007) predict the capacity of a single stone column in infinite soil mass, which does not consider the effect of spacing. It is clear from the Fig. 18, Ambily and Gandhi (2007) chose the ratio of spacing between columns to diameter of column as 1.5 and 4 based on unit cell concept while in this present study this ratio was chosen as 6 (d_c = 10 cm) and 12 (d_c = 5 cm).

6. Limitations

Several limitations should be mentioned. The models created in this study were based on data obtained from stone column loading tests in cohesive soils, with a plate diameter of 5 cm and 10 cm. The further testing and verification is recommended for the use of these models in other soils or with significantly larger plate diameters. It is well known that full-scale loading test results are valid, especially for in-situ conditions and for soil properties in which the test was performed. However, a full-scale loading test is not economic, due to the expensive cost in terms of time and money that is required for the construction, instrumentation and testing. Therefore, small-scale model test studies are widely used as an alternative to full-scale loading tests, despite of their scale-errors (Kaya and Ornek 2013, Dickin and Nazir 1999).

7. Conclusions

This study is focused directly on performance of stone columns encased with geogrid reinforcement using 2D FE program PLAXIS and physical laboratory modeling. Experiments are carried out by loading the column area alone in the unit cell area. The numerical analysis was validated by the load settlement behavior obtained from experimental test. The results of the numerical analysis based on different parameters such as effect of diameter of stone column, crushed stone's friction angle, the rigidity of geogrid and length of geogrid reinforcement are presented to quantify the effect of confinement and the mechanism for improvement in load capacity due to encasement. Based on the results, the following main conclusions can be drawn.

- Numerical analysis, using a simple constitutive model (Mohr–Coulomb model), gave results that closely match those from experimental tests for short-term stability.
- The bearing capacity of clay deposits can be increased by using stone column. Besides, the performance of the stone column can be further improved by encasing with geogrid. In case of the geogrid encasement, it is found that the bearing capacity of the stone column is increased and the lateral bulging is minimized.
- The bearing capacity of the stone column (SC) and geogrid encased stone column (GESC) increases by the increases of the column diameter. In addition, it increases with increases in crushed stone's friction angle.
- The benefit of geogrid encasement increases with decreases in the diameter of the stone columns.
- The rigidity of geogrid plays an important role in enhancing the capacity and stiffness of the encased columns. As the rigidity of geogrid increases, bearing capacity of the stone column increases and lateral bulging decreases. The bearing capacity performance of stone column increases almost linearly from EA = 0 kN/m to EA = 160-250 kN/m. After rigidity of EA = 160-250 kN/m, the bearing capacity performance of stone column remains constant. In addition, maximum lateral bulging performance of stone column increases almost linearly from EA = 0 kN/m to roughly EA = 1500 kN/m. After rigidity of roughly EA = 1500 kN/m, the maximum lateral bulging performance of stone column remains constant.

- The bearing capacity decreases by the decrease of the geogrid encasement length. In addition, maximum lateral bulging decreases with the geogrid encasement length increases. Besides, maximum lateral bulging of the stone column for different encasement length case was observed to occur roughly beneath the base of the encasement. The encasement at the top portion of the stone column (where roughly maximum lateral bulging occurs) is sufficient for the improved performance of the stone column. It is observed that, encasing stone column up to a depth equal to almost 0.5 times the height of stone column sufficiently improve the stone column.
- A similar behavior was observed when compared with existing studies. The existing studies (except Ambily and Gandhi 2007) predict the capacity of a single stone column in infinite soil mass, which does not consider the effect of spacing. But, Ambily and Gandhi (2007) chose the ratio of spacing between columns to diameter of column as 1.5 and 4 based on unit cell concept while in this present study this ratio chose as 6 (d_c = 10 cm) and 12 (d_c = 5 cm).

Nevertheless, the investigation is considered to have provided a useful basis for further research leading to an increased understanding of the application of geogrid encased stone column behavior.

References

Adalier, K., Elgamal, A., Meneses, J. and Baez, J.I. (2003), "Stone columns as liquefaction countermeasure in non-plastic silty soils", *Soil Dyn. Earthq. Eng.*, **23**(7), 571-584.

Adayat, T. and Hanna, T.H. (1991), "Performance of vibro-columns in collapsible soils", *Proceedings of Indian Geotechnical Conference on Geotechnical Analysis*, *Practice and Performance*, Surat, India, December, pp. 383-386.

Ambily, A.P. and Gandhi, S.R. (2007), "Behavior of stone columns based on experimental and FEM analysis", *J. Geotech. Geoenviron. Eng.*, **133**(4), 405-415.

Andreou, P. and Papadopoulos, V. (2006), "Modelling stone columns in soft clay", *Proceeding of the 6th European Conference on Numerical Methods in Geotechnical Engineering*, Graz, Austria, September, pp. 777-780.

ASTM D 2166 (2003), Standard test method for unconfined compressive strength of cohesive soil, *Annual book of ASTM Standards*; *American Society for Testing and Materials*, PA, USA, pp. 1-6.

ASTM D 2435-96 (1998), Standard test method for one-dimensional consolidation properties of soils, *Annual Book of ASTM standards*; *American Society for Testing and Materials*, PA, USA, pp. 207-216.

ASTM D 3080-98 (2003), Standard test method for direct shear test of soils under consolidated drained conditions, *Annual Book of ASTM Standards*; *American Society for Testing and Materials*, PA, USA, pp. 347-352.

Barksdale, R.D. and Bachus, R.C. (1983), "Design and Construction of Stone Columns Volume I", Federal Highway Administration Report FHWA. RD-83/026; *National Technical Information Service*, Springfield, VA, USA.

Black, J.A., Sivakumar, V., Madhav, M.R. and Hamill, G.A. (2007), "Reinforced stone columns in weak deposits: laboratory model study", *J. Geotech. Geoenviron. Eng.*, **133**(9), 1154-1161.

Brinkgreve, R.B.J., Broere, W. and Waterman, D. (2004), "Plaxis finite element code for soil and rock analysis", 2D –Version 8.6.

Demir, A. (2011), "Analysis of shallow foundations on reinforced granular fill over soft clay deposit", Ph.D. Dissertation; Cukurova University, Adana, Turkey.

Demir, A. and Ok, B. (2015), "Uplift response of multi-plate helical anchors in cohesive soil", *Geomech. Eng.*, *Int. J.*, **8**(4), 615-630.

Dickin, E.A. and Nazir, R. (1999), "Momentcarrying capacity of short pile foundations in cohesionless soil", *J. Geotech. Geoenviron. Eng., ASCE*, **125**(1), 1-10.
Gniel, J. and Bouazza, A. (2009), "Improvement of soft soils using geogrid encased stone columns", *Geotext. Geomembr.*, **27**(3), 167-175.
Gniel, J. and Bouazza, A. (2010), "Construction of geogrid encased stone columns: a new proposal based on laboratory testing", *Geotext. Geomembr.*, **28**(1), 108-118.
Goughnour, R.R. (1983), "Settlement of vertically loaded stone columns in soft ground", *Proceeding of the 8th European Conference on Soil Mechanics, and Foundations Engineering*, Helsinki, Finland, May, pp. 235-240.
Greenwood, D.A. (1970), "Mechanical improvement of soils below ground surfaces", *Proceeding of the Ground Engineering Conference on Institution of Civil Engineers*, London, UK, June, pp. 11-22.
Han, J. and Ye, S.L. (2002), "A theoretical solution for consolidation rates of stone column-reinforced foundations accounting for smear and well resistance effects", *The Int. J. Geomech.*, **2**(2), 135-151.
Hughes, J.M.O. and Withers, N.J. (1974), "Reinforcing of soft soils with stone columns", *Ground Eng.*, **7**(3), 42-49.
Hughes, J.M.O., Withers, N.J. and Greenwood, D.A. (1976), "A field trial of reinforcing effect of stone column in soil", *Proceeding of the Ground Treatment by Deep Compaction, Institution of Civil Engineers*, London, UK, March, pp. 32-44.
Isaac, D.S. and Girish, M.S. (2009), "Suitability of different materials for stone column construction", *Electro. J. Geotech. Eng.*, **14**, 2-12.
Kabir, M.H. and Alamgir, M. (1989), "Geotextile and geogrid jacketed stone columns in clays. Reinforced soil and geotextiles", *Proceeding of the First Indian Geotextiles Conference on Reinforced Soil and Geotextiles*, Bombay, India, December, pp. F45-50.
Kaya, N. and Ornek, M. (2013), "Experimental and numerical studies of t-shaped footings", *Acta Geotechnica Slovenica*, **10**(1), 43-58.
Latifi, N., Rashid, A.S.A., Siddiqua, S. and Majid, M.Z.A. (2016a), "Strength measurement and textural characteristics of tropical residual soil stabilised with liquid polymer", *Measurement*, **91**, 46-54.
Latifi, N., Horpibulsuk, S., Meehan, C.L., Majid, M.Z.A. and Rashid, A.S.A. (2016b), "Xanthan gum biopolymer: an eco-friendly additive for stabilization of tropical organic peat", *Environ. Earth Sci.*, **75**(9), 1-10.
Latifi, N., Marto, A. and Eisazadeh, A. (2016c), "Experimental investigations on behaviour of strip footing placed on chemically stabilised backfills and flexible retaining walls", *Arab. J. Sci. Eng.*, **41**(10), 4115-4126.
Madhav, M.R. and Miura, N. (1994), "Soil improvement. Panel report on stone columns", *Proceeding of the 13th International Conference on Soil Mechanics and Foundation Engineering*, New Delhi, India, January, **Volume 5**, pp. 163-164.
Malarvizhi, S.N. and Ilamparuthi, K. (2004), "Load versus settlement of clay bed stabilized with stone and reinforced stone columns" *Proceeding of GeoAsia–2004*, Seoul, Korea, June, pp. 322-329.
Marto, A., Latifi, N., Janbaz, M., Kholghifard, M., Khari, M., Alimohammadi, P. and Banadaki, A.D. (2012), "Foundation size effect on modulus of subgrade reaction on sandy soils", *Electr. J. Geotech. Eng.*, **17**, 2523-2530.
Marto, A., Moradi, R., Helmi, F., Latifi, N. and Oghabi, M. (2013), "Performance analysis of reinforced stone columns using finite element method", *Electr. J. Geotech. Eng.*, **18**, 315-323.
McKelvey, D., Sivakumar, V., Bell, A. and Graham, J. (2004), "Modelling vibrated stone columns in soft clay", *Proceedings of the ICE-Geotechnical Engineering*, **157**(3), 137-149.
Mitchell, J.K. and Huber, T.R. (1985), "Performance of a stone column foundation", *J. Geotech. Eng.*, **111**(2), 205-223.
Mitra, S. and Chattopadhyay, B.C. (1999), "Stone columns and design limitations", *Proceeding of the Indian Geotechnical Conference*, Calcutta, India, December, pp. 201-205.
Mohamad, E.T., Latifi, N., Marto, A., Moradi, R. and Abad, S.V.A.N.K. (2013), "Effects of relative density on shear strength characteristics of sand-tire chips mixture", *Electr. J. Geotech. Eng.*, **18**, 623-632.

Murugesan, S. and Rajagopal, K. (2006), "Geosynthetic-encased stone columns: numerical evaluation", *Geotext. Geomembr.*, **24**(6), 349-358.

Murugesan, S. and Rajagopal, K. (2009), "Studies on the behavior of single and group of geosynthetic encased stone columns", *J. Geotech. Geoenviron. Eng.*, **136**(1), 129-139.

Priebe, H.J. (1995), "The design of vibro replacement", *Ground Eng.*, **28**(10), 31-37.

Rao, B.G. and Bhandari, R.K. (1980), "Skirting a new concept in design of heavy storage tank foundation", *Proceedings of the 6th Southeast Asian Conference on Soil Engineering*, Taipei, Taiwan, May, pp. 283-300.

Sathish, S., Yadav, O.P. and Deepak, M. (1997), "Soft ground improvement using stone columns – A field trial", *Proceeding of the Indian Geotechnical* Conference, Vadodara, India, December, pp. 311-314.

Wehr, J. (2006), "The undrained cohesion of the soil as criterion for the column installation with a depth vibrator", *Proceeding of the International Symposium on Vibratory Pile Driving and Deep Soil Vibratory Compaction*, *TRANSVIB*, Paris, September, pp. 157-162.

Wood, D.M., Hu, W. and Nash, D.F.T. (2000), "Group effects in stone column foundations: Model tests", *Geotechnique*, **50**(6), 689-698.

Yoo, C. and Kim, S.B. (2009), "Numerical modeling of geosynthetic-encased stone column-reinforced ground", *Geosynth. Internat.*, **16**(3), 116-126.

CC